Black carbon health impacts in the Indo-Gangetic plain: Exposures, risks, and mitigation

Shubha Verma, Sanhita Ghosh, Olivier Boucher, Rong Wang, Laurent Menut

ATMOSPHERIC SCIENCE

Black carbon health impacts in the Indo-Gangetic plain: Exposures, risks, and mitigation

Shubha Verma[1]*, Sanhita Ghosh[1], Olivier Boucher[2], Rong Wang[3], Laurent Menut[4]

A large discrepancy between simulated and observed black carbon (BC) surface concentrations over the densely populated Indo-Gangetic plain (IGP) has so far limited our ability to assess the magnitude of BC health impacts in terms of population exposure, morbidity, and mortality. We evaluate these impacts using an integrated modeling framework, including successfully predicted BC concentrations. Population exposure to BC is notable, with more than 60 million people identified as living in hotspots of BC concentration (wintertime mean, >20 μg m^{-3}). The attributable fraction of the total cardiovascular disease mortality (CVM) burden to BC exposures is 62% for the megacity. The semiurban area comprised about 49% of the total BC-attributable CVM burden over the IGP. More than 400,000 lives can potentially be saved from CVM annually by implementing prioritized emission reduction from the combustion of domestic biofuel in the semiurban area, diesel oil in transportation, and coal in thermal power plant and brick kiln industries in megacities.

INTRODUCTION

Black carbon (BC) aerosols are mainly emitted from incomplete combustion processes, whether it is from combustion engines in the automobile sector, residential burning of wood and coal, industrial power stations using heavy oil or coal, field burning of agricultural wastefs, or forest and vegetation fires. Recent studies of the health effect of airborne particles show a strong association of combustion-derived particles, specifically BC, with cardiovascular disease (CVD) mortality (CVM) (*1*, *2*). BC may not be itself a toxic component of fine particulate matter (PM), but it is known to be co-emitted with toxic compounds, which are by-products of incomplete combustion of fuel and can adhere to the BC fractal morphology. BC may thus operate as a universal carrier of a wide variety of chemicals of varying toxicity into the lungs. These chemicals can then come in contact with the body's major defense cells and the systemic blood circulation (*3*). Recent studies also indicate that health risks (per unit aerosol mass) of CVM and CVD morbidity are as much as 6 to 26 times larger for BC than for undifferentiated PM (*1*, *4*, *5*). There is thus value in specifically targeting BC emission abatement. BC, therefore, serves as a valuable air quality indicator, reflecting the health risks of airborne particles to effectively protect public health from the combustion PM.

Furthermore, the spatial and temporal distributions of BC concentration over the Indian region are very heterogeneous in comparison to undifferentiated PM mass (*6*). This is attributable to a large number of local combustion sources of BC, while PM also includes other species such as desert dust, which comes, in part, from long-range transport over most of the Indian subcontinent during the summer season and western India during the winter season (*6*). This heterogeneity may lead to a contrast in population exposure to BC compared to total PM mass. The World Health Organization (WHO) (*3*) suggested that BC should serve as an additional indicator to $PM_{2.5}$ (PM with aerodynamic diameters ≤ 2.5 μm) to quantify human exposure to airborne pollution and assess the health effects of such exposure, with consequences on how to evaluate the local or regional mitigation measures to reduce the population exposed to combustion aerosols.

The Indo-Gangetic plain (IGP) region over the Indian subcontinent is known as one of the global hot spots of atmospheric pollutants with very large concentrations of BC aerosols in wintertime (*7*–*9*). Within India, this region also has the largest population density, with area types, e.g., rural to megacity (refer to table S2). Epidemiological studies provide evidence of an association between short-term exposure to elevated ambient air pollution (such as that during wintertime) and a higher risk of acute CVD, with systemic oxidative stress induced by air pollution as a potential underlying mechanism (*1*, *10*, *11*).

To estimate the magnitude of BC-attributable health impacts concerning population exposure, morbidity, and mortality and targeting BC emission abatement for health benefits, an integrated modeling framework as implemented in the present study is shown in Fig. 1. We obtain a spatially and temporally fine resolved gridded distribution of surface BC concentration for the wintertime over the IGP through BC transport simulations in a chemical transport model [CHIMERE (*12*)]. Simulating atmospheric BC concentration is necessary to provide information on BC aerosols over large areas where atmospheric measurements are sparse, particularly in rural and remote locations comprising a low population density and experiencing relatively less anthropogenic pollution than urban or megacity sites.

RESULTS

BC distribution over the IGP

Spatial distribution (10 × 10 km^2) of BC surface concentration for all-day and daytime BC concentration averaged over the winter months (November to December) from the simulations are presented in Fig. 2 (A and B and C, respectively). Two simulation experiments, namely, "$constrained_{simu}$" and "$baseline_{simu}$," are carried out by implementing the two emission datasets in CHIMERE, respectively. These datasets are baseline BC emission and observationally constrained

[1]Department of Civil Engineering, Indian Institute of Technology Kharagpur, Kharagpur 721302, India. [2]Institut Pierre-Simon Laplace, CNRS/Sorbonne Université, 75252 Paris Cedex 05, France. [3]Department of Environmental Science and Engineering, Fudan University, Shanghai 200433, China. [4]Laboratoire de Météorologie Dynamique, IPSL, CNRS/Ecole Polytechnique/Sorbonne Université/Ecole Normale Supérieure, 91128 Palaiseau Cedex, France.
*Corresponding author. Email: shubha@iitkgp.ac.in

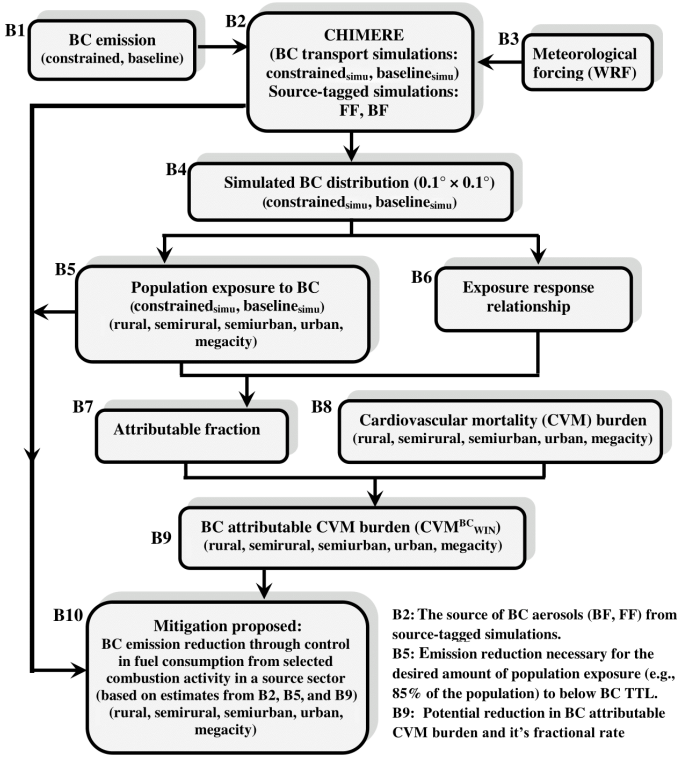

Fig. 1. Integrated modeling framework. Flowchart of the methodology to estimate the magnitude of BC-attributable health impacts and mitigation strategies targeting sustainable BC emission reduction for health benefits. The various blocks in the flowchart are enumerated as B1, B2, B3, ..., B10. BF, biofuel; FF, fossil fuel; TTL, theoretical threshold limit; WRF, Weather Research and Forecasting model. The BC health impact metrics and the proposed mitigation analyzed domain-wide for area types (rural, semirural, semiurban, urban, and megacity) are marked in specific blocks.

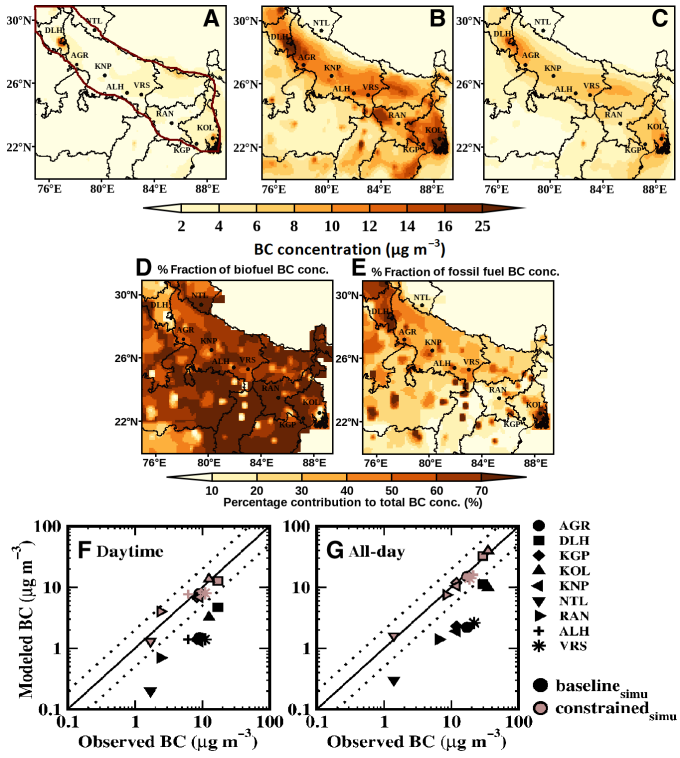

Fig. 2. Modeled BC distribution, sources of BC, and model versus measurements. Spatial distribution (10 × 10 km^2) of the wintertime averaged modeled BC surface concentration (in μg m^{-3}) from (**A**) baseline$_{simu}$ for all-day values and (**B** and **C**) constrained$_{simu}$ for (B) all-day and (C) daytime values. Fractional distribution (%) of modeled BC concentration from (**D**) BF and (**E**) FF emissions. (**F** and **G**) Comparison of (F) daytime and (G) all-day wintertime mean surface BC concentration (in μg m^{-3}) between model estimates and measured counterparts at stations under study over the IGP: Agra (Agr), Delhi (DEL), Kharagpur (KGP), Kolkata (KOL), Kanpur (KNP), Nainital (NTL), Ranchi (RAN), Allahabad/Prayagraj (ALH), and Varanasi (VRS). Measured BC surface concentration is obtained at stations over the IGP from available studies (refer to the "Anthropogenic emissions and simulation experiments" section in Materials and Methods). The region bounded by the brown line in (A) represents the IGP region. The dotted lines in (F) and (G) correspond to the value within ±25% of the 1:1 comparison shown as a solid line.

or so-called constrained BC emission (refer to the "Anthropogenic emissions and simulation experiments" section in Materials and Methods). The two emission datasets are used to estimate population exposures under the scenario of simulated atmospheric BC concentration with low baseline BC emissions and that representing the present-day ambient values (close to observed) with observationally constrained BC emissions. Patch of large wintertime BC pollution mostly composed of wintertime all-day (daytime) BC surface concentration in the range of 14 to 25 (6 to 8) μg m^{-3} is obtained from constrained$_{simu}$ estimates (Fig. 2, B and C) over the IGP. A comparison of the wintertime BC surface concentration (Fig. 2, F and G) from constrained$_{simu}$ estimates shows a good agreement with measurements at stations [refer to Fig. 2 (A to C) for stations understudy] over the IGP, with the ratio of modeled to measured winter averaged all-day (daytime) concentration being near to one. The measured BC surface concentration is obtained at stations over the IGP from available studies (refer to the "Anthropogenic emissions and simulation experiments" section in Materials and Methods and references therein).

The comparison from baseline$_{simu}$ is also shown (Fig. 2, F and G) to examine the amount of the desired reduction in atmospheric BC concentration compared to the measured, thereby targeting abatement in BC pollution with the low baseline BC emissions. In this regard, BC surface concentration from baseline$_{simu}$ is accounted for 2 to 10 times lower than its measured counterparts. The BC concentrations from baseline$_{simu}$ are used in estimating population exposure for area types and potential mitigation measures in the source of BC pollutants for health benefits (refer to the "Population exposures to ambient BC concentration" and "Source of BC aerosols: Potential mitigation measures for health benefits" sections).

The normalized mean error (NME) in constrained$_{simu}$ is 16% (14%) for both the all-day (daytime) winter averaged BC concentration (refer to table S1 as a supplement), being within the uncertainty range (10 to 20%) in BC measurements (*13*, *14*). In comparison to the present study, a large discrepancy in the simulated BC distribution in global or regional chemical transport models, with the magnitude of simulated surface BC concentrations being four to nine times lower than observations, especially during winter months over the IGP, has been reported in the previous modeling studies (*6*, *15*–*17*). Low values for the NME and root mean square error (RMSE) functions as obtained in the present study from constrained$_{simu}$ indicate

that the combination of the CHIMERE model and observationally constrained BC emissions could simulate the BC distribution efficiently over the IGP. A fine-resolved wintertime BC distribution so obtained from constrained$_{simu}$ is, therefore, further used to assess the magnitude of health impacts concerning population exposures and CVM attributable to wintertime BC exposures over the IGP.

Population exposures to ambient BC concentration

To understand population exposures to BC (expressed as population number or relative percentage of population corresponding to area types in the IGP exposed to a given BC concentration), the spatial distribution of population density (10×10 km^2) with the overlay of contours of BC concentration is presented (Fig. 3, A and B). The population over the IGP is mainly spread over the semiurban area (refer to table S2) (*18*). More than 300 million people over the IGP including more than 150, 80, 20, and 35 million inhabitants over the semiurban, urban, megacities, and semirural areas, respectively, are exposed mostly to the wintertime all-day (daytime) mean BC concentration of magnitude higher than 10 (5) μg m^{-3}. The IGP population is exposed to all-day (daytime) values twice (just equivalent to) the BC theoretical threshold limit (TTL) (refer to the "Population exposure and BC-attributable disease burden over the IGP" section in Materials and Methods for details on BC TTL). Even more than 30 (4) million people over the rural area are also found exposed to the magnitude of all-day (daytime) mean BC concentration just above the TTL. More than 60 million people live over hot spots of BC concentration (Fig. 3, A and B), i.e., locations with a typically high wintertime all-day (daytime) mean BC surface concentration of magnitude larger than 20 (8) μg m^{-3} and 4 (1.6) times the TTL. Besides the megacity areas, the hot spots are identified prominently over urban areas in the eastern and northern IGP, in addition, to that over semiurban and a few semirural locations, thereby indicating that the large value of BC pollutants is present even for the rural/semirural population belts, though, with a low population density and that

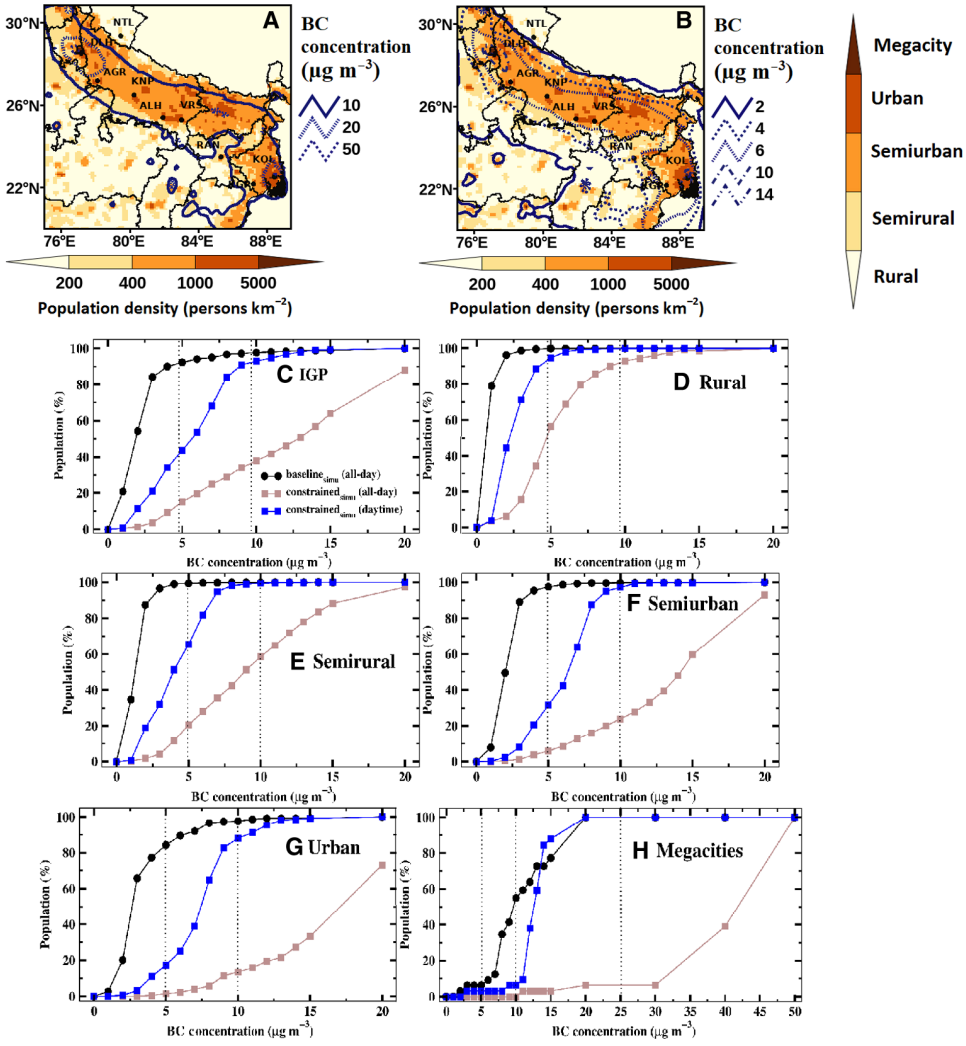

Fig. 3. Spatially mapped population density with contours of BC concentration and area-wide cumulative population exposures to BC. Spatial distribution of population density (number of inhabitants per square kilometer) overlaid with contours of wintertime averaged modeled BC concentration for (**A**) all-day and (**B**) daytime values. The area types corresponding to population density are also shown on a color scale at the extreme right. Cumulative population exposure (%) to BC concentration from baseline$_{simu}$ (black line) and constrained$_{simu}$ (brown line and blue line) for the (**C**) entire IGP and area types of (**D**) rural, (**E**) semirural, (**F**) semiurban, (**G**) urban, and (**H**) megacity.

with a low BC emission rate. Notably, the BC emission rate for rural/semirural population belts is lower by 15 times and 2 to 4 times the emission rates for megacity and semiurban/urban areas, respectively (refer to table S2). About 12 million people over the two megacities of the IGP (population density of >5000 people per km^{-2}) are exposed to the extreme levels of wintertime all-day (daytime) BC concentration of magnitude as large as 40 μg m^{-3} (12 μg m^{-3}). The population-weighted averages (refer to table S2) of the wintertime all-day (daytime) BC surface concentrations for the urban belt and the megacity are larger by about 3 times (1.5 to 1.8 times) and 8 times (3 times), respectively, than the rural belt.

BC concentrations from $constrained_{simu}$ and $baseline_{simu}$ against the cumulative percentage of population distribution are presented in Fig. 3 (C to H). These figures are shown considering both the overall population of the IGP (Fig. 3C) and the populations corresponding to area types over the IGP (Fig. 3 (D to H)). More than 85% of the population over the IGP (Fig. 3C) is exposed to all-day mean BC concentration above the TTL, with about 36% being exposed to more than triple the TTL. The cumulative distribution pattern is generally observed to exhibit an S-shaped curvature for all the area types, which indicates the exponential increase in population exposures and that toward a higher range of BC concentration from rural to megacities. The exponential increase for the all-day mean $constrained_{simu}$ BC concentration is visualized at values larger than 5, 10, and 30 μg m^{-3} for semirural or semiurban, urban, and megacities, respectively. The exponential increase for the daytime mean $constrained_{simu}$ BC concentration is at values larger than 5 μg m^{-3} for semiurban or urban, 10 μg m^{-3} for megacities while being below 5 μg m^{-3} for rural and semirural.

Analysis of the cumulative percentage population exposure for each of the area types (Fig. 3, D to H) shows that more than 90% (>70%) of the semiurban, urban population, and megacity populations are exposed to all-day (daytime) mean BC concentration above the TTL. The exposure is significant, as this corresponds to 70% of the semiurban and urban population being exposed to all-day mean BC concentration of value greater than two to four times the TTL and 94% of the megacity population to greater than four times the TTL. The BC exposure level is high for the semirural and rural population as well, with about 79 and 43%, respectively, of their population being exposed to the all-day mean of BC surface concentration above the TTL. The BC exposure for the population corresponding to these area types, though, appears to be better, considering the daytime mean than the all-day mean, with about 90% of the rural and 70% of the semirural population being exposed to daytime mean BC concentration of value within the TTL. The population exposure for all area types, except megacities, is found to be relatively acceptable with the $baseline_{simu}$ experiment (Fig. 3, C to H), for which more than 85% of the population is exposed to BC concentration below the TTL.

Thus, the above analyses indicate the extent of reduction (by a factor of 8 or by 87%) in the BC emissions (as perceived from observationally constrained BC emission data representing the present-day ambient concentrations) required to make it equivalent to the low emission scenario from the $baseline_{simu}$. This reduction is necessary to bring about 85% of the population exposure to ambient BC levels of value below the TTL.

BC-attributable CVM burden and potential mitigation measures

We further evaluate the health functions over the IGP as estimated in the present study (using formulation and assumption given in the "Population exposure and BC-attributable disease burden over the IGP" section in Materials and Methods) for the CVM attributable to wintertime BC exposure. The spatial distribution of relative risk (RR) factor (Fig. 4A) indicates this being greater than one (excess risks) over the entire IGP, thereby indicating wintertime BC exposures being a potential risk factor for the entire IGP, including semirural and rural areas. Notably, no excess risk of CVM (RR ≤ 1) due to BC exposure is noted over the rural area covering most of the central India. The RR value is significantly large (1.5 to 4) over the identified BC hotspot locations, with this being the largest for the megacities, Delhi and Kolkata (3 to 4), thereby indicating the highest potential of BC exposure as a risk factor for the megacities. The spatial distribution of CVM (shown as number of inhabitant mortality), attributable to the wintertime BC exposures for each gridmesh (resolution, 10 × 10 km^2), is presented in Fig. 4B. Patches of a large BC-attributable CVM burden (>100 inhabitant mortality per gridmesh) is found spatially distributed over the BC hotspot locations, with the highest-burden (>500 to 1000 inhabitant mortality per gridmesh) observed in and around megacities (Kolkata and Delhi). The BC-attributable CVM burden is estimated as composed of 400,000 deaths annually over the entire IGP.

Of the total BC-attributable CVM burden over the IGP, the largest fraction (49%) exists for the semiurban area, followed by the urban (28%) and megacity (14%), with the lowest being for the rural (2%), followed by semirural (8%). The attributable fraction (AF) of the CVM burden to BC exposures (refer to Eq. 4 and table S2) is obtained as 62% for the megacity (including the two megacities over the IGP: Kolkata and Delhi) compared to that as 30% for the urban and 20% for the semiurban. The megacity comprises the largest BC burden among the area types and that arising primarily from fossil fuel (FF) combustion (mainly diesel combustion; discussed later). The epidemiological survey studies over India show that CVM attributable to air pollution over the megacity is the largest among area types and is found twice more significant than the rural area (*19*). An increased risk of CVM in urban areas attributable to transport-related air pollution has also been inferred in available studies over the United States and Europe (*20*–*22*). The present study over the IGP showing the increased AF of the CVM burden to BC exposures for the megacity corroborates the information from the studies mentioned above. The present study, however, insists that the large CVM burden over the urban/megacity is specifically attributable to significant BC in air pollution exposures. The above analysis thus indicates an urgent requirement of the domain-wide sustainable mitigation plan toward the reduction in the combustion PM (BC) to provide health benefits to inhabitants from BC pollution exposure. The domain-wide targeted mitigation plan is suggested because the potential emission source of BC pollutants is distinctive for the domains or area types (e.g., for the semiurban and urban/megacity), as discussed in the "Source of BC aerosols: Potential mitigation measures for health benefits" section.

To evaluate comparison of the CVM burden attributable to the wintertime BC exposures with the $PM_{2.5}$ exposures, the spatial distribution of the ratio of the CVM attributable to BC to that attributable to $PM_{2.5}$ exposures for each gridmesh (resolution, 10 × 10 km^2) is also presented in Fig. 4C. The RR (excess risks) attributable to $PM_{2.5}$ exposures (RR-$PM_{2.5}$; refer to fig. S1A) exhibits a relatively uniform distribution (1 to 1.2) over the entire area understudy, including the urban hot spots of the IGP and the rural area covering most of the central India. Unlike the RR due to BC, the RR due to

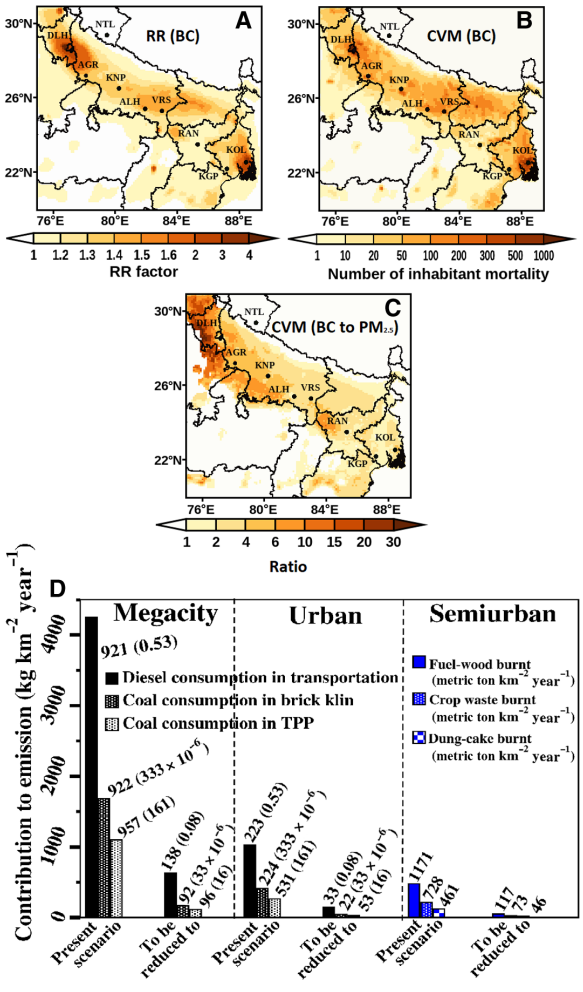

Fig. 4. Health impact functions due to BC exposures, comparison with $PM_{2.5}$ exposures, and area-wide sustainable mitigation plan. Spatial distribution (resolution, 10 × 10 km^2) of health impact functions for (**A**) RR and (**B**) CVM burden attributable to the wintertime BC exposures (shown as number of inhabitant mortality per gridmesh on color scale). The white space in (A) covering areas of central India implies no excess risk of CVM due to BC exposure over the region. (**C**) Ratio of CVM burden attributable to the wintertime BC exposures to that of $PM_{2.5}$ exposures. (**D**) Domain-wide (megacity, urban, and semiurban) sustainable mitigation plan composed of the amount of mitigation of emissions required (*x* axis) from the present scenario ($constrained_{simu}$) to the desired level ($baseline_{simu}$) for health benefits from BC health impacts through the corresponding reduction in fuel consumption for energy from identified combustion activity in a source sector. The *y* axis shows BC emission (in kg km^{-2} $year^{-1}$) arising from fuel consumption for energy (given as number on bars with units in metric ton km^{-2} $year^{-1}$). The number inside the brackets shown on the bars represents metric ton $year^{-1}$ per heavy vehicle for diesel consumption, metric ton $year^{-1}$ per 1000 bricks produced for coal consumption in brick kiln industry, and metric ton $year^{-1}$ per unit megawatt of electricity for coal consumption in thermal power plant (TPP). The fuel consumption shown corresponds to those that need priority to be reduced to maximize health benefits to the population corresponding to an area type.

$PM_{2.5}$ exposures does not distinctly represent the regions and area types with large combustion-derived PM exposures needing a prioritized air quality control. This is because unlike BC, which is a primary combustion-derived particle component of $PM_{2.5}$, most of the other abundant $PM_{2.5}$ components in the atmosphere are derived from both natural (crustal or marine) and anthropogenic sources or secondary chemical transformations (*10*). It is found that the RR attributable to BC exposures is higher (20 to 40% over most of the IGP) than RR-$PM_{2.5}$ (fig. S1B). This is typically significantly larger, being three to four times the RR-$PM_{2.5}$ over the megacities and surrounding area. The CVM burden attributable to $PM_{2.5}$ exposures is estimated to be 10 to 50 inhabitant mortality per gridmesh, with the largest number of deaths (100 to 500 inhabitant mortality per gridmesh) observed in and around megacities (Kolkata and Delhi) (fig. S1C). This also comprises 80,000 deaths over the entire IGP, being five times lower than the CVM burden attributable to BC exposures. Thus, health benefits, if planned on the basis of BC pollutants reduction over the IGP, can save about 400,000 lives from air pollution–attributable CVM over India, compared to 80,000 only if planned on the basis of $PM_{2.5}$ reduction. In comparison to that of $PM_{2.5}$ exposures, the CVM burden attributable to BC exposure is, in general, higher by two to four times (Fig. 4C), with this being as large as 10 times or more over the northern IGP (including parts of Punjab/Haryana). The spatial pattern of RR and CVM burden due to BC and $PM_{2.5}$ exposures, therefore, ascertains BC as a useful index for effective air quality management to reduce exposure to particles from combustion sources and thereby mitigate the CVM burden attributable to air pollution over the Indian subcontinent.

Furthermore, it is also noted that the AF of the CVM burden to BC exposures is estimated as 24% over the IGP, compared to that being 5% only for the $PM_{2.5}$ exposures. An available epidemiological survey study infer air pollution–attributable CVM in India as 31% (*23*), thereby indicating that the CVM burden attributable to air pollution exposures over India can be well represented by that attributable to the BC component of the air pollution. Considering that the IGP has the largest population density and comprises the largest BC burden, the BC-attributable CVM burden over the IGP closely matches the air pollution–attributable CVM in India. The CVM burden attributable to BC exposures over the IGP is about five times larger than that attributable to $PM_{2.5}$ and is found to strongly govern the air pollution–attributable CVM burden over India. The reduction of BC-attributable CVM burden over the IGP can thus be helpful to potentially regulate the elimination of the CVM burden attributable to air pollution exposures over India.

Thus, there is value in specifically targeting BC emission reduction over the Indian subcontinent for reducing the adverse health effects due to air pollution effectively. However, BC comprises a small fraction (within 15%) of the total $PM_{2.5}$ mass over most of the IGP (*24*). The increase in the CVM per unit increase in aerosol mass is, however, 15 times larger for BC than $PM_{2.5}$ over the IGP [see concentration-response coefficient per unit of BC mass concentration (β) in the "Population exposures and BC-attributable CVM burden over the IGP" section in Materials and Methods], and hence, a more significant CVM burden due to BC exposures than that due to $PM_{2.5}$ is found over the IGP. Available studies examining health effects of PM components in China (*22*, *25*) show a stronger association of combustion-derived particles, specifically BC, with CVM. As mentioned before, the CVD morbidity and CVM per unit aerosol mass are inferred as much as 6 to 26 times larger for BC than for undifferentiated PM (*1*, *4*, *5*) in epidemiological studies in the United States and China. In comparison to that over the IGP, world regions such as the United States have a low BC burden, being about 18 to 20 times lower than the $PM_{2.5}$ (*10*, *20*). Hence, unlike that found over the IGP, the RR factor and the CVM burden attributable to BC exposures are

inferred to be nearly similar to the $PM_{2.5}$ exposures in the United States–based epidemiological studies (*26*–*28*). Our study, however, suggests that health benefits, if planned on the basis of reducing the CVM burden attributable to $PM_{2.5}$ exposures over the Indian subcontinent, not only would be primarily underestimated but also would potentially miss targeting specific regions and area types with significant combustion-derived PM exposures needing a prioritized air quality control. BC as an additional indicator to $PM_{2.5}$ to quantify human exposure to airborne pollution specifically is thus required over regions where BC concentration is large, such as that over the IGP.

Source of BC aerosols: Potential mitigation measures for health benefits

To evaluate the domain-wide mitigation measures, we examine the source of BC aerosols over the IGP through an analysis of source-tagged simulation [refer to Fig. 2 (D and E)]. Wintertime BC concentration is primarily (>60%) from emissions of biofuel (BF) combustion for cooking and heating in the residential household sector over most of the IGP. The BF combustion in the residential sector (40 to 50%) and FF combustion in industrial and transportation sectors (50 to 60%) are dominant contributors to the wintertime BC concentration over the urban area in the central IGP (including Kanpur, Agra, and Varanasi). The wintertime BC concentration over the northern IGP (in and around megacity Delhi including the semirural area of Haryana) and eastern IGP (in and around megacity Kolkata) is found to mainly (>60%) originate from FF combustion.

A previous study (*29*) showed that the desired level of reduction in PM concentration was not attained for highly polluted areas (e.g., Delhi) even when considering the hypothesized sensitivity experiment using the complete abatement of residential BF combustion. The PM reduction for the Delhi region was studied on the basis of residential BF combustion abatement and without tracking the source of origin of combustion-derived PM over the Delhi region. The origin of atmospheric BC pollutants primarily from the FF combustion (and not the residential BF) over the Delhi–National Capital Region, as found in the present study, is the reason for the failure to attain the desired level of ambient PM concentration reduction in the above-mentioned previous study (*29*). This further justifies the usage of BC as a better index of combustion-derived PM. Moreover, tracking the sources of BC serves as a helpful step toward local or regional abatement of combustion PM emissions for reducing the adverse health effects due to air pollution exposures. The domain-wide mitigation measures, including primarily the BF combustion in the semiurban area and FF combustion in industrial and transportation sectors in megacities and urban areas, are thus suggested and discussed in the next paragraph.

In principle, 100% or so mitigation of BC emissions is strongly recommended. However, for sustainable attainment of health benefits, we suggest stagewise mitigation measures to achieve 87% reduction in BC emissions foremostly. The suggested reduction in emissions is required to bring more than 85% of the population exposures to the BC concentration below the TTL. The strategic mitigation measures, conceptualized domain-wide, e.g., for the semiurban, urban, and megacity (refer to Fig. 4D), are suggested. The conceptualized mitigation measures are based on prevalent emission sources of BC aerosol from the source sector and the predominant fuel combustion activity in the identified source sector (refer to the "Anthropogenic emissions and simulation experiments" section in Materials and Methods). Besides the emission source, the mitigation plan includes analysis of population exposures to BC pollution over the domain, in conjunction with the total number and fraction of population affected from CVM attributable to wintertime BC exposures (also refer to Fig. 1). The conceptualized mitigation measures suggested to be implemented for sustainable achievement of potential health benefits include, e.g., (i) mitigation of residential BF combustion activity over the entire IGP, preferentially identifying the population using fuelwood and crop waste, would lead to decreasing the CVM burden to a wider extent, saving about 220,000 lives (benefiting a large number of semiurban inhabitants spread over a wide area of the IGP, including rural and semirural). The CVM burden would decrease at a large fractional rate, saving 50,000 of 80,000 lives under CVM burden for a megacity, as well as that at a wider extent, saving 160,000 lives of a total of 400,000 deaths corresponding to CVM attributable to wintertime BC exposures over the entire IGP, through specifically targeting urban/megacity for the (ii) reduction of FF combustion sources, preferentially diesel oil combustion in transportation and coal combustion in industries. As per the above-suggested measures, to achieve an 87% reduction in the latest BC emissions (constrained) from FF combustion source for urban/megacity, the amount of BC emissions required to be reduced from diesel combustion in heavy-duty vehicles and that from coal combustion in thermal power plant (TPP) and brick kiln industries is shown in Fig. 4D. This reduction corresponds to a sevenfold decrease in the diesel consumption per square kilometer for urban and megacity, planned either by reducing the number of vehicles or curbing the amount of diesel consumed per vehicle (e.g., through switching to hybrid technology measures) by 85% (i.e., 530 kg vehicle^{-1} year^{-1} to 80 kg vehicle^{-1} year^{-1}). Furthermore, the above reduction corresponds to a 10-fold decrease in the total coal consumption in the TPP sector or coal combustion per unit megawatt of electricity generated in TPP by 90% (i.e., 160 metric ton MW^{-1} year^{-1} to 16 metric ton MW^{-1} year^{-1}). The above reduction also corresponds to a 17- and 10-fold decrease in the total coal consumption in the brick kiln sector for megacity and urban regions, respectively, or to a 90% decrease in coal consumption per 1000 bricks produced in the brick kiln (i.e., 300 to 33 g of coal per 1000 bricks produced). The amount of BC emissions required to be reduced from the combustion of fuelwood, crop waste, and dung cake in the residential household fuel used to achieve an 87% reduction in the present-day BC emissions (observationally constrained) from BF combustion source in the semiurban area is shown in Fig. 4D. This reduction corresponds to a 10-fold decrease in the consumption of the BF per square kilometer over the IGP.

The recently launched national mission, such as the Ujjawal Bharat mission of the government of India, which promotes and aids in providing clean energy combustion source preventing the residential coal and biomass fuel combustion for residential cooking, would be effective in reducing the mortality risks associated with the combustion PM over the IGP. Regulatory measures are also required for curbing BC emissions from FF combustion sources over the megacity and urban areas as per the above-suggested measures. We suggest promoting domain-wide mitigation plans based on estimating the credits for source-wide BC emission reduction and the exchange of credits among the potential source sectors, which contribute to BC emissions on a regional to national to global scale. Evaluation of these plans over the Indian region is in progress and will be presented in a future study.

DISCUSSION

In the present study, the health impacts attributable to ambient BC aerosols are assessed in terms of population exposures to BC concentration and CMV burden for the South Asia IGP. A fine-resolved wintertime BC distribution favorably representing the observed values required for the assessment is fulfilled from BC transport simulations in a high-resolution (10×10 km^2) chemical transport model (CHIMERE) using observationally constrained BC emissions for the Indian region. Population exposures to BC are significant for more than 300 million persons living in the IGP, including 94% of the megacity and 70% of semiurban/urban inhabitants exposed to wintertime BC concentration twice larger than the defined TTL. These are also inferred to be high for rural and semirural populations, with about 43 and 79%, respectively, of these populations being exposed to all-day wintertime mean BC concentration above the TTL.

The spatial mapping of the RR factor implies that all populations living in the IGP, including those in rural areas, are under the risk of BC-attributable health effects. The CVM burden attributable to BC exposures (per 10×10 km^2), including more than a hundred deaths over the BC hot spot locations and as large as a thousand deaths for the megacities of Kolkata and Delhi, is identified in the IGP. The CVM burden attributable to BC exposures over the IGP is five times larger than the undifferentiated fine PM and strongly governs the air pollution–attributable CVM burden over India. The CVM burden can be reduced by a factor of 2 to 4 times more in most of the IGP or as large as 10 times or more in the northern IGP (including parts of Punjab/Haryana) by applying control of BC pollutants than that of targeting $PM_{2.5}$ mass concentration. Our study presents BC as a valuable index for harmful combustion-derived particles. It suggests controlling the sources of BC as an effective approach to managing combustion-derived PM components to reduce the adverse health effects attributable to air pollution.

The AF of the CVM burden to BC exposures is 62% for the megacity (Kolkata and Delhi) compared to 24% for the IGP. Of the total number of lives affected from CVM attributable to BC exposures over the different area types, 49% are in the semiurban area. We find that significant exposure to atmospheric BC is a main driver of mortality by CVD in Indian megacities. Our study asserts that reducing the CVM burden attributable to BC exposures over the IGP can potentially regulate the elimination of the CVM burden attributable to air pollution exposures over India.

On the basis of our estimates of population exposures, an 87% reduction in present-day BC emissions is required to avoid the adversity of BC-attributable health impacts and save about 400,000 lives annually from BC-induced CVM over the IGP. Health benefits are potentially attainable, reducing the CVM burden by a wider extent, thereby saving about 220,000 lives of semiurban including rural populations through the preferential mitigation of the residential fuelwood and crop waste combustion. The CVM burden is estimated to decrease by a large fractional rate, saving about 50,000 lives of the megacity population (out of the CVM burden of 80,000 lives) and, by a wider extent, saving about 160,000 lives of the urban/megacity population through the preferential reduction of diesel oil combustion in transportation and coal combustion in industries, specifically TPP and brick kilns. The domain-wide mitigation plan comprising the amount of mitigation of emissions required through the corresponding reduction in fuel consumption for energy from identified combustion activity is suggested. The reduction includes the total coal consumption in the industry or consumption per unit megawatt of electricity generated in TPP or per 1000 of bricks produced in the brick kiln industry; the diesel consumption per vehicle in the transportation and biofuel use per square kilometer in the residential household sector are presented in the study.

This study provides the first evaluation of disease burden attributable to BC exposure over the Indian region using a successfully predicted BC distribution combined with consistent health functions for BC. Our study ascertains the WHO suggestion that BC should serve as an indicator, in addition to $PM_{2.5}$, to quantify human exposure to airborne pollution. We assert BC as an additional indicator is specifically required over regions with a significant BC burden such as the IGP. This study pushes policy-makers toward sustainable mitigation of emissions considering the sources of combustion PM (rather than bulk PM mass) and providing health benefits to more than 300 million persons living in the IGP exposed to enormous BC concentration above the desired TTL.

MATERIALS AND METHODS

Simulation of BC surface concentration

Simulation of surface concentration of BC aerosol is carried out using two state of the art regional deterministic models: WRF v3 for the meteorology and CHIMERE v2014b for the chemistry transport (*12*). CHIMERE being in offline mode, it is forced by WRF meteorological fields. The two models are running at the same fine grid horizontal resolution over the domain spanning from 20°N to 31°N, 75°E to 89.4°E [refer to Fig. 2 (A to C)], including the IGP region. The simulations are done at a horizontal resolution of 0.085°×0.114° (approximately 10 km by 10 km), including the number of grid points as 126 and 129 along the longitude and latitude, respectively. The grid resolution is helpful to study spatial scale characteristics of regional air pollution across the area types (megacity, urban, semiurban, and rural areas). The fine-grid resolved BC distribution is used to evaluate across the area types: (i) population exposures to BC concentration, (ii) BC-attributable CVM burden, and (iii) potential mitigation measures. The simulations are performed for the year 2015 with a spin-up time of 10 days and analyzed in the present study averaged for the winter months of November and December.

The WRF meteorological model

The WRF model (https://www2.mmm.ucar.edu/wrf/users/download/get_source.html; last accessed 20 April 2022) is a state-of-the-art numerical weather forecast and atmospheric simulation system designed for both research and operational applications. The initial and boundary meteorological conditions for WRF simulation are obtained from Global Forecast System (*30*) National Center for Environmental Prediction–FINAL operational global analysis data at a spatial resolution of 1° × 1°. The meteorological data are horizontally interpolated to the simulation grids (10 km by 10 km) internally by the WRF Preprocessing System.

The characteristics of the land surface, such as soil type, vegetation index, albedo, or surface topography, are provided by the National Center for Atmospheric Research and available at https://rda.ucar.edu/datasets/ds083.2/index.html/ (last accessed 20 April 2022). The meteorological boundary conditions, including sea surface temperature, are updated every 6 hours. The physical scheme option used for WRF simulation include the Lin scheme for the microphysics (*31*), subgrid convection by the Grell-3D scheme (*32*), the NOAH land surface module (*33*), the Yonsei University planetary boundary layer scheme (*34*), and the rapid radiative Transfer model for radiative transfer (*35*).

The CHIMERE chemistry-transport model

CHIMERE is a regional chemistry-transport model dedicated to simulating tens of gaseous and aerosols species (*12*). In this study, the model version 2014b is used. The aerosol module in CHIMERE provides hourly concentrations of 10 chemical species: sulfates, nitrates, ammonium, primary organic and BC, secondary organic aerosols, sea salt, natural and anthropogenic dust, and water (*36*). Aerosols are represented with 10 bins, with mean mass median diameters ranging from 0.05 to 40 μm. Radiation and photolysis is calculated online using the FastJX module (*37*). In this study, the focus will be done on BC concentrations only. The simulated $PM_{2.5}$ concentration in CHIMERE is also used while presenting a comparison of the BC health impacts with that of $PM_{2.5}$.

Horizontal transport is solved with the van Leer scheme (*38*) and with a time step of 10 min. Vertically, mixing is diagnosed from vertical velocity, and diffusion follows a classical K_z approach (*12*). Boundary layer height is diagnosed using the scheme of Troen and Mart (*39*), and deep convection fluxes are calculated using the scheme of Tiedtke (*40*). The deposition module of the model includes both wet and dry deposition processes for aerosols (*41*). Boundary conditions are determined by monthly climatologies of global chemistry transport model Laboratoire de Météorologie Dynamique Atmospheric General Circulation Model (LMDZT-GCM) coupled to the Interactions between Aerosols and Chemistry model (*42*). Meteorological fields required by CHIMERE as input (e.g., three-dimensional wind, air temperature, and relative humidity) are provided from those simulated at an hourly rate in the WRF model.

Anthropogenic emissions and simulation experiments

BC transport simulations are conducted with the two BC emission datasets in CHIMERE (at a spatial resolution 0.25° × 0.25° over India) including (i) recently estimated observationally constrained or so-called constrained BC emission [annual BC emission rate of 2534 Gg $year^{-1}$ (*16*)] over the Indian region and (ii) extracted baseline BC emission from forward BC simulation (*43*) in the LMDZT-GCM [annual BC emission rate of 388 Gg $year^{-1}$ (*44*–*46*)]. The wintertime BC emission flux across area types (megacity, urban, semiurban, semirural, and rural) over the study domain from constrained and baseline emissions are also given in table S2. The BC emission flux across area types from the constrained emission database is found to be seven to nine times larger than the baseline. As also mentioned previously, the purpose to conduct $baseline_{simu}$ using baseline BC emissions in CHIMERE is to estimate population exposures under the scenario of simulated atmospheric BC concentration with low baseline BC emissions, thereby targeting abatement in BC pollution and its sources with the low baseline BC emissions.

Nevertheless, while using constrained BC emissions in a state-of-the-art chemical transport model, CHIMERE, it is a foremost requirement to obtain the adequate spatial distribution of wintertime BC distribution that favorably represents the present-day ambient values (close to observed). A previous study (*24*) examined direct radiative effects due to BC over the IGP, comparing the modeled BC distribution in CHIMERE with five new BC emission inventories. The BC emission inventories implemented in CHIMERE included constrained BC emissions and the latest bottom-up BC emissions (India-based: Smog-India; global: Coupled Model Intercomparison Project phase 6, Emission Database for Global Atmospheric Research-V4, and Peking University BC Inventory). The study showed that the modeled BC concentration using the bottom-up emission inventories in CHIMERE is, in general, two to four times lower than that observed over most of the IGP. In comparison, BC simulations with constrained BC emissions in CHIMERE could simulate the distribution of BC pollution over the IGP more efficiently than with bottom-up emissions (*24*).

In the present study, the efficacy of the CHIMERE model to simulate the wintertime BC distribution over the IGP is represented by comparing the simulated all-day and daytime (1000 h to 1600 h local time) BC concentration averaged over the winter months (November to December) with their observed counterparts from measurements at stations over the IGP. Measured BC surface concentrations as obtained from available studies at stations over the IGP and used for model comparison include those at Agra (*47*), Delhi (*48*), Kharagpur (Research group, IIT Kharagpur), Kolkata (*49*), Kanpur (*50*), Nainital (*13*), Ranchi (*51*), Allahabad/Prayagraj (*52*), and Varanasi (*53*). The location of station understudy within various area types is represented in Fig. 3A, i.e., megacity (Kolkata, Delhi), urban (Agra, Kanpur, Allahabad/Prayagraj, Varanasi), semiurban (Kharagpur, Ranchi), and semirural (Nainital). Our study presents model comparison with available measurements at stations widespread across the IGP and covering almost all area types in the IGP. The statistical evaluation, including NME and RMSE in modeled values, is provided in the Supplementary Materials (refer to table S1). The fine grid resolved (10 km by 10 km) $constrained_{simu}$ (using constrained BC emissions in CHIMERE), which simulates successfully the wintertime BC distribution over the IGP, is used in the assessment of health burden attributable to wintertime BC exposures.

Besides the above-mentioned simulations, source-tagged BC simulations are also carried out using constrained BC emissions in CHIMERE. This is done to examine the relative contribution of BC emission source to atmospheric BC concentration and evaluate the source-based mitigation of emissions for area types (e.g., megacity, urban, and semiurban) over the IGP through the corresponding reduction in fuel consumption for energy from identified selected combustion activity in a source sector (Fig. 1). In the source-tagged BC simulations, the BC aerosol transport and atmospheric processes are simulated, implementing BC emissions in CHIMERE for each of the source sectors, including residential BF and FF combustion, with emissions outside that source sector being switched off. For the BF and FF source sectors, on estimating the relative composition (%) of BC emission from various fuel combustion activities for energy, it is seen that this composition in BF source sector comprises BC emissions primarily from the combustion of residential fuelwood (50%), followed by that of crop waste (20%), dung cake, and forest biomass (10% each) for cooking and heating in the residential household sector. For the FF source sector, this is mainly from the combustion of diesel oil (59%) in transportation, followed by coal combustion (40%, composed of 23% from brick kiln industry and 17% from the TPP). The above estimation includes the merging of the information on emission composition of the source sector with the total constrained BC emissions, information on activity-wide BC emission factor as that used in bottom-up emissions in $baseline_{simu}$, and that on fuel consumption for combustion activity for energy from the survey data of the government of India (*54*, *55*), including the report from the Department of Agriculture and Cooperation, MoA, land records and survey report, and government of West Bengal.

Population exposures and BC-attributable CVM burden over the IGP

To assess the BC-attributable health impacts, we estimate the population exposure to ambient BC aerosols and the CVM burden

attributable to wintertime BC exposure. For the spatial mapping of the population exposure to ambient BC, the gridded distribution of BC surface concentration is overlaid on a population density distribution map for the IGP region. The population density distribution is available at a spatial resolution of 10×10 km^2 (same as that of the simulated BC concentration) from census 2011 (*18*). The spatial distribution of the wintertime mean of BC surface concentration estimated over the IGP from the constrained$_{simu}$ is further used to calculate gridded distributions of the health impact function parameters like the RR, the AF, and burden of disease attributable to wintertime BC exposure. The RR is the ratio of the risk of disease or death among the exposed to the risk among the unexposed (*56*). The exposed includes the population subjected to the supposed cause of a disease or risk factor, i.e., BC exposures above the minimum threshold, and the unexposed includes the population who are not subjected to likewise the risk factor. In other words, when the RR associated with an agent or a circumstance (here BC exposures) is larger than 1, then the agent is called a risk factor.

The RR is thus a measure of the excess risk relative to the baseline risk (RR = 1). Health impact assessments, in general, set the RR to 1 (i.e., no excess risk) when the exposure is below the minimum threshold. In the present study, the RR corresponding to BC exposure is calculated in each gridmesh (resolution, 10×10 km^2) according to the Eq. 1 (*20*, *57*). If the value of RR over a given gridmesh is estimated as less than or equal to 1, then it implies no excess risk of disease or death due to BC exposure or BC exposure is not a risk factor of the CVM.

$$\mathrm{RR} = e^{\beta \Delta x} \tag{1}$$

where β is the concentration-response coefficient per unit of BC mass concentration, which represents the increase in the health risk per unit increase in BC concentration, Δx in microgram per cubic meter is the excess concentration beyond the TTL. In the present study, health impact function parameters are estimated for the CVM attributable to wintertime BC exposure (i.e., the number of people in a population who die as a result of CVD attributable to large BC exposures in winter, with RR > 1). The value of β is estimated on the basis of information from epidemiological studies providing evidence of an association between daily mortality (from CVD) and BC exposures for cooler months (*10*). This value is obtained as 0.0214 per μg m^{-3} of BC with an uncertainty of 43%. To provide a comparison of health functions for BC with that for $PM_{2.5}$, we also estimate the RR estimated for $PM_{2.5}$ exposure (RR-$PM_{2.5}$) using Eq. 1. The value of concentration-response coefficient per 1 μg m^{-3} of $PM_{2.5}$ (β for $PM_{2.5}$) is obtained as 0.0014 and is estimated in the same way as done for BC based on information from epidemiological studies providing evidence of an association between daily mortality (from CVD) and $PM_{2.5}$ mass concentration for cooler months (*10*). The ratio of β for BC to that for $PM_{2.5}$ over the IGP is obtained as 15, implying the increase in health risk estimates of CVM per unit increase in aerosol mass concentration is 15 times larger for BC than $PM_{2.5}$.

The focus to consider health impact associated with CVM in the present study is consistent with the information that CVD is now the leading cause of mortality in India with a substantial (31%) of CVM burden attributable to air pollution (*23*). The age-standardized CVM rate in India is also found to be about 16% higher than the global average (*19*). It may be noted that β is based on the information of CVM associations with exposures to BC concentration from epidemiological studies performed in the United States. Taking into account that the causes of CVM would be more comparable globally than the all-cause mortality since causes of death would differ across world regions (*58*, *59*), and because of the lack of epidemiological information including association between the CVM burden and BC exposures over the Indian region, estimating β from U.S.-based epidemiological studies is thus a useful compromise.

The uncertainty in CVM attributable to BC exposures is estimated to be about 48% (based on uncertainty in β, simulated BC concentration and mortality rate (y_0) as mentioned in Materials and Methods), which is mainly due to the uncertainty in β. Since β represents concentration-response coefficient per unit of mass concentration of BC; β with the included uncertainty would, nevertheless, represent reasonably well the health function estimates (RR factor, AF, and the CVM burden) attributable to BC exposures over the Indian region. In this regard, a comparison of estimates of RR corresponding to given BC exposures, in addition to that due to PM exposures over the IGP, using the logarithmic model (Eq. 1) from the present study have been found to be in conformity with estimates of RR (for ischemic heart disease mortality) due to PM exposure using integrated exposure-response (IER) model (*60*). The comparison with IER estimates is made corresponding to 10 times of respective BC concentration, considering health risk estimates for CVM (per unit mass) are seven to eight times larger for BC than PM (*20*).

In Eq. 1, Δx (spatially resolved at 10×10 km^2) is estimated as

$$\Delta x = C - C_0 \tag{2}$$

where C_0 is the TTL, which is the value below which there is no noticeable adverse health effects, assumed to be 5 μg m^{-3} of BC exposure, and C is the wintertime mean BC concentration at the 10×10 km^2 horizontal resolution expressed in microgram per square meter. It may be noted that the air quality standards for PM are based on 24-hour mean mass concentration of PM measured as PM_{10} or $PM_{2.5}$ (PM with aerodynamic diameters ≤ 10 μm or 2.5 μm), which are respectively 50 and 25 μg m^{-3} (*3*). The minimum threshold is, in general, determined by the epidemiological studies that provide the exposure-outcome associations. There are no air quality standards for BC concentration, but available studies consider health effect estimates corresponding to BC as for 1 μg m^{-3} of ambient BC concentration per 10 μg m^{-3} of PM_{10} (*20*). The TTL for BC is judiciously assumed, though, is subjectively driven based on inferences from available studies (i.e., one-tenth of the air quality standard for 24-hour mean mass concentration of PM_{10}). Also, the TTL considered is consistent with the average ambient BC surface concentration during clean environmental conditions (southwest monsoon rainy season) in an urban location (e.g., Kolkata), which is obtained from measurements as 5 μg m^{-3} (*49*). The TTL is found to lie within the range of all-day mean BC concentration (2 to 8 μg m^{-3}) estimated over the relatively less polluted rural area (refer to Fig. 2B) during wintertime. The TTL is also considered to be reasonable over the IGP region from the perspective that population exposures are seen to be exponentially increasing at mean BC concentration above 5 μg m^{-3} for almost all area types, including the semiurban area (Fig. 3, D to H). It is to be noted that the semiurban area comprises the largest number of the population over the IGP and has the largest fraction (49%) of the total BC-attributable CVM burden for the entire IGP. However, more than 50% of the population for the rural area type is exposed to all-day mean BC concentration below 5 μg m^{-3} and the

rural area comprises the lowest relative fraction (2%) of the total BC-attributable CVM burden for the entire IGP. The TTL of BC thus suggested as 5 μg m^{-3} in our study is found to be reasonably justified for regions (e.g., IGP) with a large BC burden.

Furthermore, the AF, the fraction of excess risk of CVM attributable to wintertime BC exposures, is estimated. The AF is calculated for each grid at the same resolution according to the following equation

$$AF = \frac{RR - 1}{RR} \quad (3)$$

The CVM burden attributable to the wintertime BC exposure (CVM_{BC}^{WIN}) is then estimated as

$$CVM_{BC}^{WIN} = y_0 \times AF \times PD \times a \quad (4)$$

where y_0 is the age-standardized mortality rate (deaths per 100,000 people in a year) due to CVD, AF is the AF due to wintertime BC exposure, PD is the gridded population density in the unit of 100,000 people per km^2, and a is the area of the gridmesh (in square kilometer). The y_0 is obtained from available burden of CVD in India from epidemiological survey studies (*19*, *23*). The y_0 for the rural/semirural, urban/semiurban, and megacity area types over India is reported as 241, 360, and 414 deaths per 100,000 people in a year (2010), respectively. The y_0 used correspond to the mortality rate due to CVD for rural type (Andhra Pradesh), urban/semiurban (Kerala), and megacity (Mumbai) as presented in the above-mentioned refereed studies. The mortality rate due to CVD for entire India was inferred as 272 deaths per 100,000 people with an uncertainty of 5% (*19*, *23*). The spatial distribution of CVM attributable to wintertime BC exposures is shown in Fig. 4B. The BC-attributable CVM burden integrated for each of the area types over the IGP is also given in table S2. The spatial distribution of RR-$PM_{2.5}$, the ratio of RR attributable to BC exposures with that to RR-$PM_{2.5}$, and CVMs attributable to the wintertime $PM_{2.5}$ exposure over the study region are also provided as fig. S1 (A to C).

SUPPLEMENTARY MATERIALS

Supplementary material for this article is available at https://science.org/doi/10.1126/sciadv.abo4093

REFERENCES AND NOTES

1. Y. Li, D. K. Henze, D. Jack, B. H. Henderson, P. L. Kinney, Assessing public health burden associated with exposure to ambient black carbon in the United States. *Sci. Total Environ.* **539**, 515–525 (2016).
2. J. Cao, H. Xu, Q. Xu, B. Chen, H. Kan, Fine particulate matter constituents and cardiopulmonary mortality in a heavily polluted Chinese City. *Environ. Health Perspect.* **120**, 373–378 (2012).
3. N. A. Janssen, M. E. Gerlofs-Nijland, T. Lanki, R. O. Salonen, F. Cassee, G. Hoek, P. Fischer, B. Brunekreef, M. Krzyzanowski, *Health Effects of Black Carbon* (WHO Regional Office for Europe, 2012).
4. B. Ostro, *Outdoor Air Pollution: Assessing the Environmental Burden of Disease at National and Local Levels* (World Health Organization, 2004).
5. F. Laden, J. Schwartz, F. E. Speizer, D. W. Dockery, Reduction in fine particulate air pollution and mortality: Extended follow-up of the Harvard Six Cities study. *Am. J. Respir. Crit. Care Med.* **173**, 667–672 (2006).
6. D. B. Kumar, S. Verma, O. Boucher, R. Wang, Constrained simulation of aerosol species and sources during pre-monsoon season over the Indian subcontinent. *Atmos. Res.* **214**, 91–108 (2018).
7. U. Paliwal, M. Sharma, J. F. Burkhart, Monthly and spatially resolved black carbon emission inventory of India: Uncertainty analysis. *Atmos. Chem. Phys.* **16**, 12457–12476 (2016).
8. V. Ramanathan, G. Carmichael, Global and regional climate changes due to black carbon. *Nat. Geosci.* **1**, 221–227 (2008).
9. S. N. Tripathi, S. Dey, V. Tare, S. K. Satheesh, S. Lal, S. Venkataramani, Enhanced layer of black carbon in a north Indian industrial city. *Geophys. Res. Lett.* **32**, L12802 (2005).
10. B. Ostro, W.-Y. Feng, R. Broadwin, S. Green, M. Lipsett, The effects of components of fine particulate air pollution on mortality in California: Results from CALFINE. *Environ. Health Perspect.* **115**, 13–19 (2007).
11. A. S. Shah, K. K. Lee, D. A. McAllister, A. Hunter, H. Nair, W. Whiteley, J. P. Langrish, D. E. Newby, N. L. Mills, Short term exposure to air pollution and stroke: Systematic review and meta-analysis. *BMJ* **350**, h1295 (2015).
12. L. Menut, B. Bessagnet, D. Khvorostyanov, M. Beekmann, N. Blond, A. Colette, I. Coll, G. Curci, G. Foret, A. Hodzic, S. Mailler, F. Meleux, J.-L. Monge, I. Pison, G. Siour, S. Turquety, M. Valari, R. Vautard, M. G. Vivanco, CHIMERE 2013: A model for regional atmospheric composition modelling. *Geosci. Model Dev.* **6**, 981–1028 (2013).
13. U. C. Dumka, K. K. Moorthy, R. Kumar, P. Hedge, R. Sagar, P. Pant, N. Singh, S. S. Babu, Characteristics of aerosol black carbon mass concentration over a high altitude location in the Central Himalayas from multi-year measurements. *Atmos. Res.* **96**, 510–521 (2010).
14. S. Verma, S. Pani, S. Bhanja, Sources and radiative effects of wintertime black carbon aerosols in an urban atmosphere in east India. *Chemosphere* **90**, 260–269 (2013).
15. X. Pan, M. Chin, R. Gautam, H. Bian, D. Kim, P. R. Colarco, T. L. Diehl, T. Takemura, L. Pozzoli, K. Tsigaridis, S. Bauer, N. Bellouin, A multi-model evaluation of aerosols over South Asia: Common problems and possible causes. *Atmos. Chem. Phys.* **15**, 5903–5928 (2015).
16. S. Verma, D. M. Reddy, S. Ghosh, D. B. Kumar, A. K. Chowdhury, Estimates of spatially and temporally resolved constrained black carbon emission over the Indian region using a strategic integrated modelling approach. *Atmos. Res.* **195**, 9–19 (2017).
17. P. Ajay, B. Pathak, F. Solmon, P. K. Bhuyan, F. Giorgi, Obtaining best parameterization scheme of RegCM 4.4 for aerosols and chemistry simulations over the CORDEX South Asia. *Climate Dynam.* **53**, 329 (2019).
18. C. Chandramouli, R. General, *Provisional Population Totals. Government of India, New Delhi - 110011* (Census Population 2022 Data, 2011), pp. 409–413.
19. D. Prabhakaran, P. Jeemon, A. Roy, Cardiovascular diseases in India. *Circulation* **133**, 1605–1620 (2016).
20. N. A. H. Janssen, G. Hoek, M. Simic-Lawson, P. Fischer, L. van Bree, H. ten Brink, M. Keuken, R. W. Atkinson, H. R. Anderson, B. Brunekreef, F. R. Cassee, Black carbon as an additional indicator of the adverse health effects of airborne particles compared with PM10and PM2.5. *Environ. Health Perspect.* **119**, 1691–1699 (2011).
21. D. Brugge, J. L. Durant, C. Rioux, Near-highway pollutants in motor vehicle exhaust: A review of epidemiologic evidence of cardiac and pulmonary health risks. *Environ. Health* **6**, 23 (2007).
22. M. Krzyzanowski, G. Bundeshaus, M. L. Negru, M. C. Salvi, *Particulate Matter Air Pollution: How it Harms Health* (World Health Organization, 2005).
23. D. Prabhakaran, P. Jeemon, M. Sharma, G. A. Roth, C. Johnson, S. Harikrishnan, R. Gupta, J. D. Pandian, N. Naik, A. Roy, R. S. Dhaliwal, D. Xavier, R. K. Kumar, N. Tandon, P. Mathur, D. K. Shukla, R. Mehrotra, K. Venugopal, G. A. Kumar, C. M. Varghese, M. Furtado, P. Muraleedharan, R. S. Abdulkader, T. Alam, R. M. Anjana, M. Arora, A. Bhansali, D. Bhardwaj, E. Bhatia, J. K. Chakma, P. Chaturvedi, E. Dutta, S. Glenn, P. C. Gupta, S. C. Johnson, T. Kaur, S. Kinra, A. Krishnan, M. Kutz, M. R. Mathur, V. Mohan, S. Mukhopadhyay, M. Nguyen, C. M. Odell, A. M. Oommen, S. Pati, M. Pletcher, K. Prasad, P. V. Rao, C. Shekhar, D. N. Sinha, P. N. Sylaja, J. S. Thakur, K. R. Thankappan, N. Thomas, S. Yadgir, C. S. Yajnik, G. Zachariah, B. Zipkin, S. S. Lim, M. Naghavi, R. Dandona, T. Vos, C. J. L. Murray, K. S. Reddy, S. Swaminathan, L. Dandona, The changing patterns of cardiovascular diseases and their risk factors in the states of India: The Global Burden of Disease Study 1990-2016. *Lancet Glob. Health* **6**, e1339–e1351 (2018).
24. S. Ghosh, S. Verma, J. Kuttippurath, L. Menut, Wintertime direct radiative effects due to black carbon (BC) over the Indo-Gangetic Plain as modelled with new BC emission inventories in CHIMERE. *Atmos. Chem. Phys.* **21**, 7671–7694 (2021).
25. X. Wang, R. Chen, X. Meng, F. Geng, C. Wang, H. Kan, Associations between fine particle, coarse particle, black carbon and hospital visits in a Chinese city. *Sci. Total Environ.* **458-460**, 1–6 (2013).
26. E. F. Kirrane, T. Luben, A. Benson, E. Owens, J. Sacks, S. Dutton, M. Madden, J. Nichols, A systematic review of cardiovascular responses associated with ambient black carbon and fine particulate matter. *Environ. Int.* **127**, 305–316 (2019).
27. T. J. Luben, J. L. Nichols, S. J. Dutton, E. Kirrane, E. O. Owens, L. Datko-Williams, M. Madden, J. D. Sacks, A systematic review of cardiovascular emergency department visits, hospital admissions and mortality associated with ambient black carbon. *Environ. Int.* **107**, 154–162 (2017).
28. S. Vedal, M. J. Campen, J. D. McDonald, T. V. Larson, P. D. Sampson, L. Sheppard, C. D. Simpson, A. A. Szpiro, National Particle Component Toxicity (NPACT) initiative report on cardiovascular effects. *Res. Rep. Health Eff. Inst.* , 5–8 (2013).

29. S. Chowdhury, S. Dey, S. Guttikunda, A. Pillarisetti, K. R. Smith, L. D. Girolamo, Indian annual ambient air quality standard is achievable by completely mitigating emissions from household sources. *Proc. Natl. Acad. Sci. U.S.A.* **116**, 10711–10716 (2019).
30. E. Kalnay, S. J. Lord, R. D. McPherson, Maturity of operational numerical weather prediction: Medium range. *Bull. Am. Meteorol. Soc.* **79**, 2753–2769 (1998).
31. Y. L. Lin, R. D. Farley, H. D. Orville, Bulk parameterization of the snow field in a cloud model. *J. Climate Appl. Met.* **22**, 1065–1092 (1983).
32. G. Grell, A. D. Devenyi, A generalized approach to parameterizing convection combining ensemble and data assimilation techniques. *Geophys. Res. Lett.* **29**, 1693 (2002).
33. F. Chen, J. Dudhia, Coupling an advanced land surface–hydrology model with the Penn State–NCAR MM5 modeling system. Part I: Model implementation and sensitivity. *Mon. Weather Rev.* **129**, 569–585 (2001).
34. S. Y. Hong, Y. Noh, J. Dudhia, A new vertical diffusion package with an explicit treatment of entrainment processes. *Mon. Weather Rev.* **134**, 2318–2341 (2006).
35. E. J. Mlawer, S. J. Taubman, P. D. Brown, M. J. Iacono, S. A. Clough, Radiative transfer for inhomogeneous atmospheres: RRTM, a validated correlated-k model for the longwave. *J. Geophys. Res.* **102**, 16663–16682 (1997).
36. B. Bessagnet, A. Hodzic, R. Vautard, M. Beekmann, S. Cheinet, C. Honoré, C. Liousse, L. Rouil, Aerosol modeling with CHIMERE—Preliminary evaluation at the continental scale. *Atmos. Environ.* **38**, 2803–2817 (2004).
37. O. Wild, X. Zhu, M. J. Prather, Fast-J: Accurate simulation of in- and below-cloud photolysis in tropospheric chemical models. *J. Atmos. Chem.* **37**, 245–282 (2000).
38. B. van Leer, *J. Comput. Phys.* **23**, 276 (1979).
39. I. Troen, L. Mahrt, A simple model of the atmospheric boundary layer; sensitivity to surface evaporation. *Bound.-Lay. Meteorol.* **37**, 129–148 (1986).
40. M. Tiedtke, A comprehensive mass flux scheme for cumulus parameterization in large-scale models. *Mon. Weath. Rev.* **117**, 1779–1800 (1989).
41. L. Zhang, S. Gong, J. Padro, L. Barrie, A size-segregated particle dry deposition scheme for an atmospheric aerosol module. *Atmos. Environ.* **35**, 549–560 (2001).
42. S. Szopa, G. Foret, L. Menut, A. Cozic, Impact of large scale circulation on European summer surface ozone and consequences for modelling forecast. *Atmos. Environ.* **43**, 1189–1195 (2009).
43. S. Verma, C. Venkataraman, O. Boucher, Attribution of aerosol radiative forcing over India during the winter monsoon to emissions from source categories and geographical regions. *Atmos. Environ.* **45**, 4398–4407 (2011).
44. M. S. Reddy, C. Venkataraman, Inventory of aerosol and sulphur dioxide emissions from India: I—Fossil fuel combustion. *Atmos. Environ.* **36**, 677–697 (2002a).
45. M. S. Reddy, C. Venkataraman, Inventory of aerosol and sulphur dioxide emissions from India. Part II—Biomass combustion. *Atmos. Environ.* **36**, 699–712 (2002b).
46. M. S. Reddy, O. Boucher, A study of the global cycle of carbonaceous aerosols in the LMDZT general circulation model. *J. Geophys. Res.* **109**, D14 (2004).
47. P. D. Safai, S. Kewat, G. Pandithurai, P. S. Praveen, K. Ali, S. Tiwari, P. S. P. Rao, K. B. Budhawant, S. K. Saha, P. C. S. Devara, Aerosol characteristics during winter fog at Agra, North India. *J. Atmos. Chem.* **61**, 101–118 (2008).
48. D. Ganguly, A. Jayaraman, H. Gadhavi, Physical and optical properties of aerosols over an urban location in western India: Seasonal variabilities. *J. Geophys. Res.* **111**, (2006b).
49. S. K. Pani, S. Verma, Variability of winter and summertime aerosols over eastern India urban environment. *Atmos. Res.* **137**, 112–124 (2014).
50. K. Ram, M. Sarin, S. Tripathi, Inter-comparison of thermal and optical methods for determination of atmospheric black carbon and attenuation coefficient from an urban location in northern India. *Atmos. Res.* **97**, 335–342 (2010a).
51. K. Lipi, M. Kumar, Aerosol and black carbon properties during different seasons in eastern part of India. *Middle-East J. Sci. Res.* **21**, 1677–1688 (2014).
52. K. V. S. Badarinath, K. M. Latha, T. R. K. Chand, R. R. Reddy, K. R. Gopal, L. S. S. Reddy, K. Narasimhulu, K. R. Kumar, Black carbon aerosols and gaseous pollutants in an urban area in North India during a fog period. *Atmos. Res.* **85**, 209–216 (2007).
53. B. P. Singh, S. Tiwari, K. P. Hopke, R. S. Singh, D. S. Bisht, A. K. Srivastava, R. K. Singh, U. C. Dumka, A. K. Singh, B. N. Rai, M. K. Srivastava, Seasonal inhomogeneity of soot particles over the central Indo-Gangetic Plains, India: Influence of meteorology. *J. Meteorol. Res.* **29**, 935–949 (2015).
54. MoSPI, *Statistical Year Book* (Central Statistics Office, Ministry of Statistics and Programme Implementation, Government of India, 2018).
55. MoSPI, *Energy Statistics* (Central Statistics Office, Ministry of Statistics and Programme Implementation, Government of India, 2018).
56. M. Porta, *A Dictionary of Epidemiology* (Oxford Univ. Press, 2014).
57. D. Krewski, M. Jerrett, R. T. Burnett, R. Ma, E. Hughes, Y. Shi, M. C. Turner, C. A. Pope III, G. Thurston, E. E. Calle, M. J. Thun, B. Beckerman, P. DeLuca, N. Finkelstein, K. Ito, D. K. More, K. B. Newbold, T. Ramsay, Z. Ross, H. Shin, B. Tempalski, Extended follow-up and spatial analysis of the American Cancer Society study linking particulate air pollution and mortality. *Res. Rep. Health Eff. Inst.* **140**, 191193 (2009).
58. S. C. Anenberg, K. Talgo, S. Arunachalam, P. Dolwick, C. Jang, J. J. West, Impacts of global, regional, and sectoral black carbon emission reductions on surface air quality and human mortality. *Atmos. Chem. Phys.* **11**, 7253–7267 (2011).
59. J. Lelieveld, J. S. Evans, M. Fnais, D. Giannadaki, A. Pozzer, The contribution of outdoor air pollution sources to premature mortality on a global scale. *Nature* **525**, 367–371 (2015).
60. R. T. Burnett, C. A. Pope III, M. Ezzati, C. Olives, S. S. Lim, S. Mehta, H. H. Shin, G. Singh, B. Hubbell, M. Brauer, H. R. Anderson, K. R. Smith, J. R. Balmes, N. G. Bruce, H. Kan, F. Laden, A. Prüss-Ustün, M. C. Turner, S. M. Gapstur, W. R. Diver, A. Cohen, An integrated risk function for estimating the global burden of disease attributable to ambient fine particulate matter exposure. *Environ. Health Perspect.* **122**, 397–403 (2014).

Acknowledgments

Funding: This work was supported through a grant received for the project National Carbonaceous Aerosol Programme–Carbonaceous Aerosol Emissions, Source Apportionment and Climate impacts (NCAP-COALESCE) from the Ministry of Environment, Forest, and Climate Change [14/10/2014-CC (Vo.II)], government of India at the Indian Institute of Technology Kharagpur (IIT-KGP). Simulations were performed in a high-performance computing cluster developed at the IIT-KGP supported through the NCAP-COALESCE. S.G. and S.V. acknowledge K. V. Prasad's (a Master's student supervised by S.V. at IIT-KGP) contribution to calculations and model setup and help in the literature review in initiating this paper. **Author contributions:** S.V. planned and coordinated the study and wrote the paper. S.G. under the supervision of S.V. conducted the BC transport simulations, performed calculations of health impact function parameters, emission reduction, and produced figures. O.B. advised throughout the paper's preparation and analysis of results and contributed to writing and completion of this paper. R.W. contributed to the writing of the paper. L.M. advised and checked for the technicality of the CHIMERE model configuration and contributed to the paper. All authors contributed to the manuscript. **Competing interests:** The authors declare that they have no competing interests. **Data and materials availability:** Most data needed to evaluate the conclusions in the paper are present in the paper and/or the Supplementary Materials. The data and materials introduced for creating figures in the manuscript are also openly available at the website: www.facweb.iitkgp.ac.in/~shubhaverma/BC-health-burdendata.html (last accessed 20 April 2022). The Weather Research and Forecasting (WRF) model is available at www2.mmm.ucar.edu/wrf/users/download/get_source.html (last accessed 20 April 2022). The chemistry-transport model "CHIMERE" is available at www.lmd.polytechnique.fr/chimere/ (last accessed 20 April 2022).

Submitted 9 February 2022
Accepted 21 June 2022
Published 5 August 2022
10.1126/sciadv.abo4093

ScienceAdvances

Black carbon health impacts in the Indo-Gangetic plain: Exposures, risks, and mitigation

Shubha Verma, Sanhita Ghosh, Olivier Boucher, Rong Wang, and Laurent Menut

Sci. Adv. **8** (31), eabo4093. DOI: 10.1126/sciadv.abo4093

Science Advances (ISSN 2375-2548) is published by the American Association for the Advancement of Science. 1200 New York Avenue NW, Washington, DC 20005. The title *Science Advances* is a registered trademark of AAAS.